A Study of Brush Seal Oil Pressure Profile Including Temperature-Viscosity Effects

E. Tolga Duran[1] and Mahmut F. Aksit[2]
Sabanci University, Istanbul, Turkey, 34956

After proven performance in air applications, brush seals are being considered for oil and oil mist sealing in aero-engines, turbines and generators. The viscous medium between the high speed rotor surface and bearing surfaces formed by brush seal bristle tips generates a hydrodynamic lifting force that determines seal clearance and leakage rate in oil sealing applications. Hydrodynamic lift force and seal clearance have strong dependence on oil temperature and viscosity. In a previous study, short bearing theory has been applied to a single bristle to obtain a solution for hydrodynamic lift force developing at a bristle tip. Rather than individual bristles, this work evaluates pressure for the bristle rows. Applying the Reynolds bearing theory to the control volume between bristle tips and the rotor surface fluid pressure distribution is obtained under each bristle row. Effective temperature and effective viscosity approach has been adopted. Pressure distribution for each bristle row in the rotor axial direction is evaluated. Then, pressure profiles for each bristle row are combined to yield the axial pressure profile under the entire brush pack.

Nomenclature

BH	=	free bristle height
β	=	constant for viscosity relation for a given oil
C, C_2	=	integration constants
c_p	=	specific heat at constant pressure
E	=	elasticity modulus of the bristle
g_x	=	gravitational acceleration in x-direction
g_y	=	gravitational acceleration in y-direction
g_z	=	gravitational acceleration in z-direction
H	=	hydrodynamic lift clearance
L	=	circumferential length of the rotor
μ	=	dynamic viscosity
$\mu_{eff\text{-}z}$	=	dynamic viscosity at certain z-coordinate
μ_{eff}	=	effective dynamic viscosity
η	=	integration factor
P	=	pressure
P^*	=	normalized pressure
P_u	=	upstream pressure
P_d	=	downstream pressure
ΔP	=	pressure difference between upstream and downstream sides
R_b	=	bristle radius
R_{rotor}	=	rotor radius
Re	=	Reynolds number
ρ	=	density
T	=	temperature
T_u	=	upstream temperature
T_d	=	downstream temperature

[1] PhD candidate, Faculty of Eng. and Natural Sci., Sabanci University, Istanbul etolgaduran@su.sabanciuniv.edu, Student member
[2] Assoc. Prof., Faculty of Eng. and Natural Sci., Sabanci University, Istanbul, aksit@sabanciuniv.edu, Member

T_{eff} = effective temperature
θ = cant angle
u = rotor surface speed
v_x = velocity of the fluid in x-direction
v_y = velocity of the fluid in y-direction
v_z = velocity of the fluid in z-direction
v_x^* = normalized velocity of the fluid in x-direction
v_y^* = normalized velocity of the fluid in y-direction
v_z^* = normalized velocity of the fluid in z-direction
w = width of the bristle pack
W = hydrodynamic lifting force
x, y, z = spatial coordinate direction

I. Introduction

Around bearings and oil sumps, tight clearance control is required to avoid oil contamination of the downstream turbine components, or to minimize oil consumption levels. In some generator applications, these requirements are accentuated by the presence of explosive cooling gas. Commonly, labyrinth seals, carbon seals or oil rings are used for bearing and oil sump sealing locations. Recently, brush seal is emerging as a viable alternative in both oil and oil mist sealing after successful secondary flow applications. A brush seal is a set of fine diameter wires densely packed between retaining and backing plates. Backing plate supports bristles under axial pressure load. Brush seals perform very well under rotor transients owing to the inherent compliance of bristles.

Majority of available literature on thermal aspects of brush seals deal with air as the sealing medium, and studies frictional heat related problems at rotor-bristle contacts. On the other hand, when a liquid medium needs to be sealed such as hydrogen generator buffer oil seals or liquid hydrogen/oxygen seals in rocket turbo pumps, problem gets more complicated as hydrodynamic lift prevents bristle rotor contact, and shear heating becomes dominant. Attempts for oil and oil mist sealing applications are rather new starting with Ingistov [1], who reported use of brush seal in a bearing oil sealing application. Later, Bhate et al. [2] reported success in similar gas turbine bearing oil sealing application. They were first to report data on brush seal oil coking tests. In a later publication, Aksit et al. [3] demonstrated the presence of hydrodynamic lift appearing as increased oil leakage with speed. Their findings indicated that oil temperature rise stabilizes at high speeds due to shear thinning.

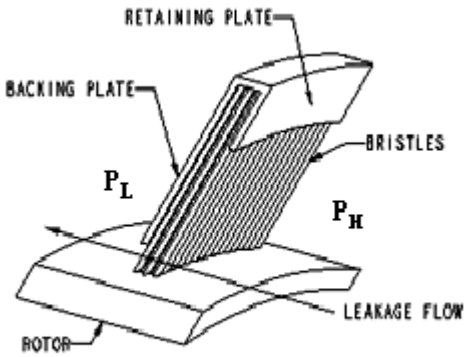

Figure 1 Brush seal geometry

To provide a better understanding about the critical balance of hydrodynamic lift force with speed, viscosity and pressure difference, an analytical study on shear heat in liquid sealing medium within the hydrodynamic lift clearance was presented by Duran et. al. [4, 5]. These works suggest a dependence of hydrodynamic lift force and seal clearance on oil temperature and viscosity. They also present an analytical solution to oil temperature rise due to shear heating. The control volume is selected as the oil between the rotor surface and the bristle pack. Pressure distribution is assumed to change linearly in the rotor axial direction [4], and thermal analysis is performed with this pressure distribution. Removing the constant pressure gradient assumption results in pressure and temperature distribution close to the results of analysis using linear pressure profile [5]. Experimental studies suggest almost constant pressure gradient in the rotor axial direction. This is consistent with the earlier analysis results of Duran et al. [4, 5]. In this study, pressure distribution is calculated for the control volume which is selected as the oil under each bristle by applying Reynolds bearing theory. Pressure distribution for each bristle row is evaluated by including the effect of temperature rise. Cyclic pressure distribution is assumed for the bristles in the rotor tangential direction. Once the pressure profiles under each bristle row is obtained including temperature-viscosity effect, these profiles are combined to yield the pressure profile under the brush pack.

II. Selection of the control volume and boundary conditions

Selection of control volume is important since it defines the valid region for the derived pressure distribution. For hydrodynamic bearing theory, control volume for each bristle is selected as given in Fig. 2. A local coordinate system is defined for each control volume of interest. The subscript in the coordinate system stands for the bristle number. The indexing set as to define the first bristle at the upstream side, and the last bristle at the downstream side. Number of bristles in one row of the bristles is defined by n_r, which generally changes between ten and sixteen. For the brush seal of interest, n_r is 16.

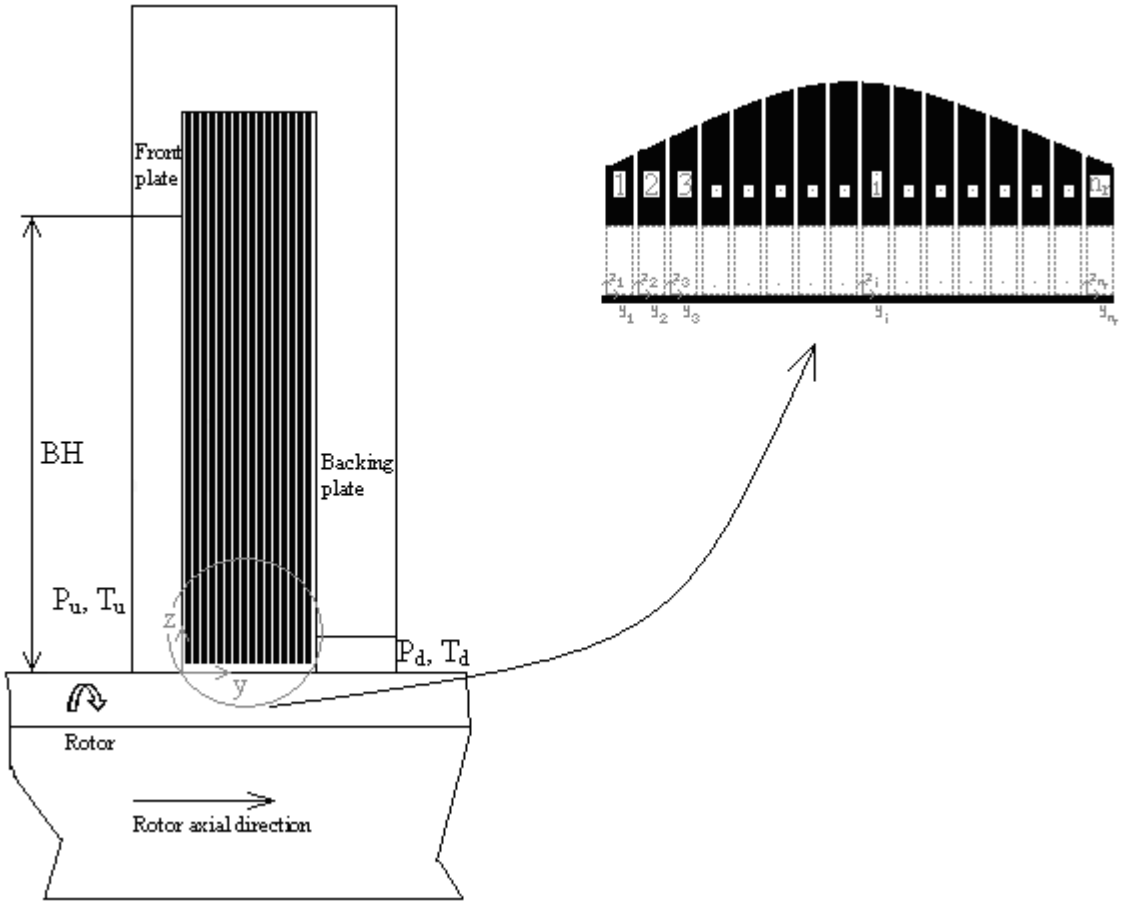

Figure 2 Selection of control volume for each bristle

For the sake of simplicity, and due to the fact that axial leakage flow is dominant, radial flows (flows in z-direction in Fig. 2) are neglected in this study. In order to find the pressure distribution, Reynolds bearing theory is applied with the assumptions given below.

1. Steady state
2. Incompressible flow
3. Radial flows are neglected due to the fact that the axial flow is dominant.
4. Convection from rotor surface and bristle surfaces to the fluid is neglected.

Rotor and bristle surfaces are taken as unwrapped flat surfaces. As illustrated in Fig. 3, h_i is the distance between the rotor and i^{th} bristle surface, and defined by Hertizian contact of two cylinders with inclined axes, as in Eq. 1.

$$h_i = H + \frac{x_i^2}{2R_{eq}} + \frac{y_i^2}{2R_b} \tag{1}$$

H is the hydrodynamic lift clearance and it is assumed to be the same for every bristle. R_{eq} is the equivalent bristle bending curvature, and R_b is the bristle radius. Hydrodynamic lift clearance and equivalent bristle bending curvature are assumed to be the same for each bristle. Value of bristle radius for the brush seal of interest is 0.051 mm. Selection of the local coordinate for the i^{th} bristle is illustrated in Fig. 3. Since front plate tightly clamps the brush pack, bristles are assumed to be supported from the free bristle height, *BH*, and they bend under the effect of

hydrodynamic lifting force generated by wedge action. Free bristle height for the current analysis is 16mm. Selection of control volume for a bristle can be observed in more detail in Fig. 3. Boundaries for *y*-coordinate are *0* and $2R_b$. The length of the bristle projection can be taken as *BH* since cant angle, Θ, is 45°. Boundaries for *x*-coordinate are *–BH* and *0*.

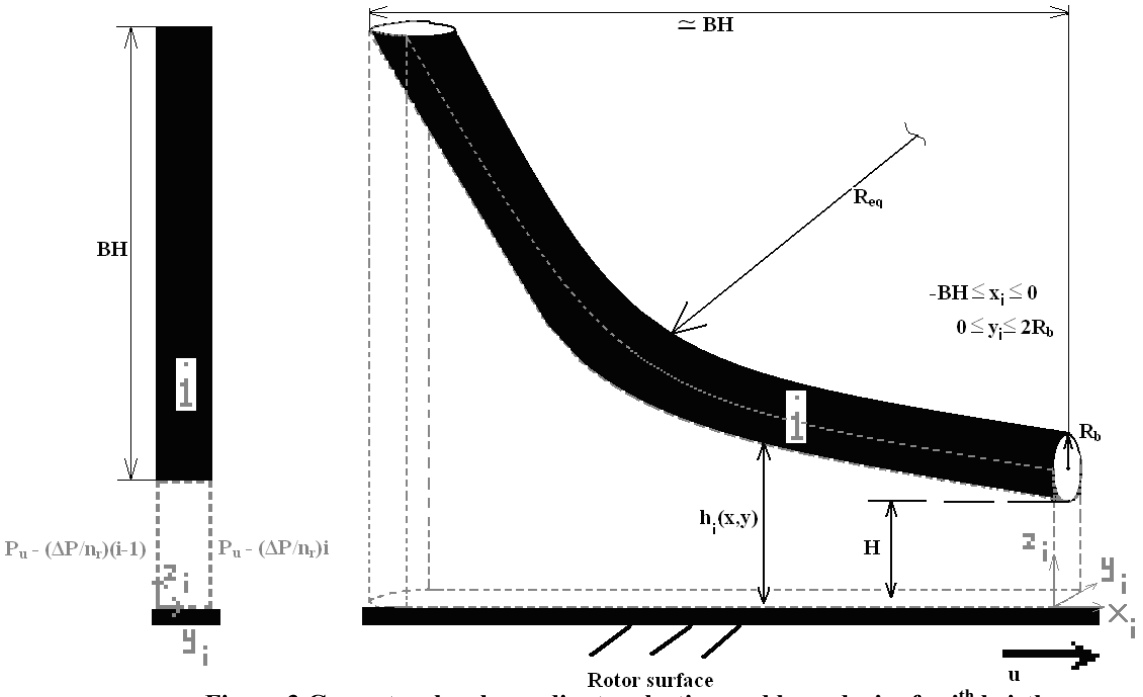

Figure 3 Geometry, local coordinate selection and boundaries for i[th] bristle

The equivalent bristle bending curvature is the radius of bristle where the radii of unwrapped rotor and bent bristle are combined. It can be calculated by using the formula,

$$\frac{1}{R_{eq}} = \frac{1}{R_{bend}} + \frac{1}{R_{rotor}} \tag{2}$$

R_{bend} is the bent bristle radius, and simply taken as equal to free bristle height. R_{rotor} is the radius of rotor with the same value given in the previous sections.

III. Application of Reynolds bearing theory for each bristle including shear heating

Temperature has significant influence on high speed lift clearance stabilization, and the effect of shear heating should be included in the analysis of brush seals. It is expected that fluid temperature increases as it travels in rotor axial direction under the brush pack. However, considering fluid viscosity as a function of speed, pressure difference and lift clearance there is no simple solution to Reynolds bearing relations. In order to simplify the problem, the approach taken here is to calculate and consider a effective temperature under each bristle row, and iteratively solve Reynolds equation with constant effective viscosity for each bristle row. Then combine the calculated fluid pressures to obtain the pressure profile for the entire pack.

Effective viscosity for each bristle row can be calculated using the effective temperature provided by Duran et. al. [4] as follows.

$$T = T_0 + \frac{1}{2\beta}\ln\left(\frac{f_1}{f_2} + f_3 \cdot f_4\right) \tag{3}$$

where

$$
\begin{aligned}
f_1 &= \exp\left(2\beta\left(T_u - T_0\right)\right) \\
f_2 &= \exp\left[\frac{\left(2z-H\right)^2}{\rho c_p\left(z^2 - zH\right)} \cdot \frac{\Delta P}{w} \cdot \beta \cdot y\right] \\
f_3 &= \frac{4\left(u \cdot w \cdot \mu_0\right)^2}{\left[H \cdot \Delta P \cdot \left(2z-H\right)\right]^2} \\
f_4 &= \exp\left[-\frac{\left(2z-H\right)^2}{\rho c_p\left(z^2 - zH\right)} \cdot \frac{\Delta P}{w} \cdot \beta \cdot y\right] - 1
\end{aligned}
\tag{4}
$$

Then, effective viscosity can be calculated by the formula,

$$\mu_{eff} = \mu_0 \cdot e^{-\beta\left(T_{eff} - T_o\right)} \tag{5}$$

where,

$$T_{eff} = \frac{1}{w}\int_0^w T_{mean-z}(y) \cdot dy \tag{6}$$

$$T_{mean-z}\left(y\right) = \frac{1}{H}\int_0^H T(y,z) \cdot dz \tag{7}$$

Reynolds bearing theory can be applied to each bristle with the assumptions given before. It is known that $Re_{H\text{-}u}$ is much smaller than unity so that inertia terms can be neglected. Reynolds equation can be stated for a typical hydrodynamic bearing formed by the i^{th} bristle as,

$$\frac{\partial}{\partial x_i}\left[h_i^3 \frac{\partial P_i}{\partial x_i}\right] + \frac{\partial}{\partial y_i}\left[h_i^3 \frac{\partial P_i}{\partial y_i}\right] = 6\mu_{eff} u \frac{dh_i}{dx_i}, \quad -BH \le x_i \le 0 \text{ and } 0 \le y_i \le 2R_b \tag{8}$$

In the above equation, x_i terms can be related with $BH=16\ mm$, and y_i terms can be related with $2R_b=0.102mm$. An order of magnitude analysis reveals that $\partial / \partial x_i$ terms can be neglected when compared with $\partial / \partial y_i$ terms, since $BH >> 2R_b$, $\partial / \partial x_i << \partial / \partial y_i$. This simplification yields the differential equation given below.

$$\frac{\partial}{\partial y_i}\left[h_i^3 \frac{\partial P_i}{\partial y_i}\right] = 6\mu_{eff} u \frac{x_i}{R_{eq}} \tag{9}$$

Boundary conditions for each bristle row *(in y-direction)* can be found using pressure load *(ΔP)* and number of bristle rows in rotor axial direction (n_r). By doing so, more realistic boundary conditions are defined and interaction between the bristles can be provided. For the first bristle, which corresponds the $y_1=0$, the left side *(Fig.2)* has the pressure value of upstream. Considering a linear pressure profile in rotor axial direction pressure drop per bristle row can simply be calculated by dividing pressure load, ΔP, to n_r. Therefore, the right (downstream) side pressure $(y_1=2R_b)$ for the the first bristle can be calculated by subtracting the pressure drop for a bristle row from upstream pressure. The upstream boundary condition for the second bristle equals to the downstream boundary condition for the first bristle, and this interaction continues until the last bristle in rotor axial direction is reached. The boundary conditions for each bristle are given below.

$$
\begin{aligned}
i, \quad y_i = 0 &\Rightarrow P_i(y_i = 0) = P_u - \frac{\Delta P}{n_r} \cdot (i-1) \\
y_i = 2R_b &\Rightarrow P_i(y_i = 2R_b) = P_u - \frac{\Delta P}{n_r} \cdot i
\end{aligned}
\tag{10}
$$

i: Changes from 1 to n_r

The inter bristle gap, d_{lb}, can be defined as the gap between two adjacent bristles. The exact value for inter bristle gap is not known. Its value changes between the one-twentieth and one-fortieth of the bristle diameter. Since the inter bristle gap is very small compared to the bristle diameter, it is neglected in this study. Applying the boundary conditions to Eq. 9 yields,

$$\frac{\partial P_i}{\partial y_i} = 6\mu_{eff} u \frac{x_i \cdot y_i}{R_{eq}} \cdot \frac{1}{\left(H + \frac{x_i^2}{2R_{eq}} + \frac{y_i^2}{2R_b} \right)^3} + C_1(x_i) \frac{1}{\left(H + \frac{x_i^2}{2R_{eq}} + \frac{y_i^2}{2R_b} \right)^3} \tag{11}$$

where $C_1(x_i)$ is integration constant. Integrating the above equation with respect to y_i yields pressure distribution as,

$$P_i = \int 6\mu_{eff} u \frac{x_i \cdot y_i}{R_{eq}} \cdot \frac{1}{\left(H + \frac{x_i^2}{2R_{eq}} + \frac{y_i^2}{2R_b} \right)^3} \partial y_i + \int C_1(x_i) \frac{1}{\left(H + \frac{x_i^2}{2R_{eq}} + \frac{y_i^2}{2R_b} \right)^3} \partial y_i + C_2(x_i) \tag{12}$$

where $C_2(x_i)$ is another integration constant. Evaluation of the integral components of the Eq. 11 is given in the following.

$$\int 6\mu_{eff} u \frac{x_i \cdot y_i}{R_{eq}} \cdot \frac{1}{\left(H + \frac{x_i^2}{2R_{eq}} + \frac{y_i^2}{2R_b} \right)^3} dy_i = \frac{6\mu_{eff} \cdot u \cdot x_i}{R_{eq}} \int \frac{y_i}{\left(H + \frac{x_i^2}{2R_{eq}} + \frac{y_i^2}{2R_b} \right)^3} dy_i$$

$$\Downarrow$$

$$\frac{6\mu_{eff} \cdot u \cdot x_i}{R_{eq}} \int \frac{y_i}{\left(H + \frac{x_i^2}{2R_{eq}} + \frac{y_i^2}{2R_b} \right)^3} dy_i = \frac{6\mu_{eff} \cdot u \cdot x_i}{R_{eq}} \cdot \left(\frac{-R_b}{2} \right) \cdot \frac{1}{\left(H + \frac{x_i^2}{2R_{eq}} + \frac{y_i^2}{2R_b} \right)^2} \tag{13}$$

and

$$\int C_1(x_i) \frac{1}{\left(H + \frac{x_i^2}{2R_{eq}} + \frac{y_i^2}{2R_b} \right)^3} dy_i = C_1(x_i) \cdot \int \frac{dy_i}{\left[\left(H + \frac{x_i^2}{2R_{eq}} \right) \cdot 2R_b + y_i^2 \right]^3 \cdot \frac{1}{8R_b^3}}$$

$$\Downarrow$$

Define a function, $\alpha_i^2 = 2R_b \cdot \left(H + \frac{x_i^2}{2R_{eq}} \right)$

$$C_1(x_i) \cdot \frac{2R_b^3}{\alpha_i^2} \cdot \left[\frac{y_i}{\left(\alpha_i^2 + y_i^2 \right)^2} + 3 \int \frac{dy_i}{\left(\alpha_i^2 + y_i^2 \right)^2} \right] =$$

$$C_1(x_i) \cdot \frac{2R_b^3}{\alpha_i^2} \cdot \left\{ \frac{y_i}{\left(\alpha_i^2 + y_i^2 \right)^2} + \frac{3}{2\alpha_i^2} \left[\frac{y_i}{\left(\alpha_i^2 + y_i^2 \right)} + \frac{1}{\alpha_i} \arctan\left(\frac{y_i}{\alpha_i} \right) \right] \right\} \tag{14}$$

Fluid pressure distribution for the i^{th} bristle can be found by substituting Eq. 13 and 14 into the Eq. 12. After the substitution, integration constants can be found by applying boundary conditions given in Eq. 10.

$$P_i = \frac{6\mu_{eff}\cdot u\cdot x_i}{R_{eq}}\cdot\left(\frac{-R_b}{2}\right)\cdot\frac{1}{\left(H+\frac{x_i^{\,2}}{2R_{eq}}+\frac{y_i^{\,2}}{2R_b}\right)^2}$$

$$+C_1(x_i)\cdot\frac{2R_b^{\,3}}{\alpha_i^{\,2}}\cdot\left\{\frac{y_i}{\left(\alpha_i^{\,2}+y_i^{\,2}\right)^2}+\frac{3}{2\alpha_i^{\,2}}\left[\frac{y_i}{\left(\alpha_i^{\,2}+y_i^{\,2}\right)}+\frac{1}{\alpha_i}\arctan\left(\frac{y_i}{\alpha_i}\right)\right]\right\}+C_2(x_i)$$

B.C's:

$$y_i = 0 \Rightarrow P_i(y_i=0) = P_u - \frac{\Delta P}{n_r}\cdot(i-1)$$

and

$$y_i = 2R_b \Rightarrow P_i(y_i=2R_b) = P_u - \frac{\Delta P}{n_r}\cdot i$$

$$\Downarrow \text{Apply BC's}$$

$$P_i = F_3 + \frac{F_2}{F_1}\cdot F_4 + F_5$$

$$F_1 = \frac{2R_b^{\,3}}{\left(\alpha_i^{\,2}\right)}\left\{\frac{2R_b}{\left(\alpha_i^{\,2}+4R_b^{\,2}\right)^2}+\frac{3}{2\alpha_i^{\,2}}\left[\frac{2R_b}{\alpha_i^{\,2}+4R_b^{\,2}}+\frac{1}{\alpha_i}\arctan\left(\frac{2R_b}{\alpha_i}\right)\right]\right\}$$

$$F_2 = \frac{-\Delta P}{n_r}-\frac{6\mu_{eff}u}{R_{eq}}x_i\left(\frac{R_b}{2}\right)\left[\frac{1}{\left(H+\frac{x_i^{\,2}}{2R_{eq}}+1\right)^2}-\frac{1}{\left(H+\frac{x_i^{\,2}}{2R_{eq}}\right)^2}\right]$$

$$F_3 = \frac{6\mu_{eff}\cdot u\cdot x_i}{R_{eq}}\cdot\left(\frac{-R_b}{2}\right)\cdot\frac{1}{\left(H+\frac{x_i^{\,2}}{2R_{eq}}+\frac{y_i^{\,2}}{2R_b}\right)^2} \qquad (15)$$

$$F_4 = \frac{2R_b^{\,3}}{\left(\alpha_i^{\,2}\right)}\left\{\frac{2R_b}{\left(\alpha_i^{\,2}+y_i^{\,2}\right)^2}+\frac{3}{2\alpha_i^{\,2}}\left[\frac{2R_b}{\alpha_i^{\,2}+y_i^{\,2}}+\frac{1}{\alpha_i}\arctan\left(\frac{y_i}{\alpha_i}\right)\right]\right\}$$

$$F_5 = P_u - \frac{\Delta P}{n_r}\cdot(i-1) - \frac{6\mu_{eff}u}{R_{eq}}x_i\left[\frac{-R_b}{2}\cdot\frac{1}{\left(H+\frac{x_i^{\,2}}{2R_{eq}}\right)^2}\right]$$

$$\alpha_i^{\,2} = 2R_b\cdot\left(H+\frac{x_i^{\,2}}{2R_{eq}}\right)$$

Pressure distribution given above includes the effect of shear heating as μ_{eff}, which is found from effective temperature. Pressure is a function of brush seal geometry (R_b, R_{eq}, n_r), pressure load (ΔP), upstream pressure (P_u), rotor surface speed (u) and hydrodynamic lift clearance (H). Experimental hydrodynamic lift clearance values of Aksit et. al. [6], which are given in Table 1, are used for the calculations.

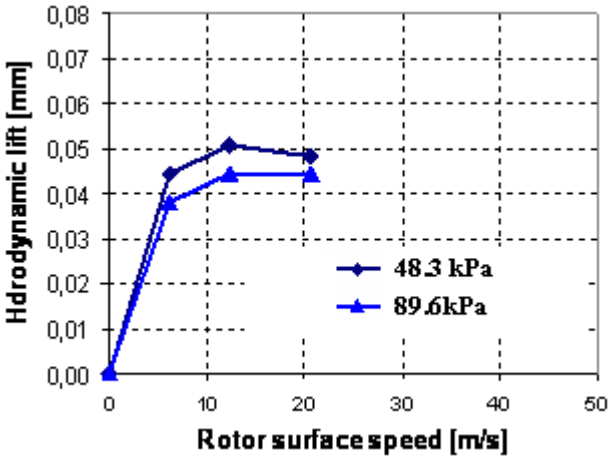

Figure 4 Hydrodynamic lift clearance versus rotor speed under different pressure loads, based on experimental leakage data Aksit et al. [6]

Table 1 Hydrodynamic lift clearances for certain rotor surface speeds at distinct pressure differences obtained from experimental leakage data, Aksit et al. [16]

	ΔP = 48.3kPa	ΔP = 89.6kPa
Rotor surface speed, u	Hydrodynamic lift clearance, H	Hydrodynamic lift clearance, H
0	0	0
6.2m/s	0.044mm	0.038mm
12.5m/s	0.052mm	0.044mm
20.5m/s	0.047mm	0.044mm

IV. Results and discussion

Pressure relation derived in Eq. 15 is a function of both x_i and y_i coordinates. Pressure distribution along x_i direction for $y_i=R_b$ *(middle of the bristle, see Fig. 3)* of each bristle is given in Fig. 5 for 48.3 kPa pressure load and 6.2 m/s rotor surface speed. Calculations are performed using MATLAB.

As it can be seen from the Fig 5, pressure change in x_i direction shows similar distribution for each bristle. Plots have the same character, but magnitudes are decreasing as going from upstream side to downstream side as expected. Oil pressure for the first bristle is around upstream pressure (P_u), whereas it is around downstream pressure $(P_d=P_a)$ for the last bristle. There is an evident change in oil pressure between -2mm and 0, which corresponds to length of projection of bristle portion at *"Fence height, FH"* onto the x_i coordinate. Beyond -7mm, oil pressure remains constant. As an example, oil pressure distributions along x_i and y_i axes are presented in Fig. 6 under 89.6kPa pressure load for 20.5m/s rotor surface speed.

Combining oil pressure change with respect to local coordinates of bristles (x_i, y_i) gives the pressure distribution under the bristle pack of one row of bristles. As it can be observed from the Fig. 6, pressure distribution along rotor axial direction is almost linear for every point in rotor tangential direction as expected. It takes the upstream pressure value for $y = 0$ *(at the upstream side)*, and drops to downstream pressure value for $y = w$ *(at the downstream side)*.

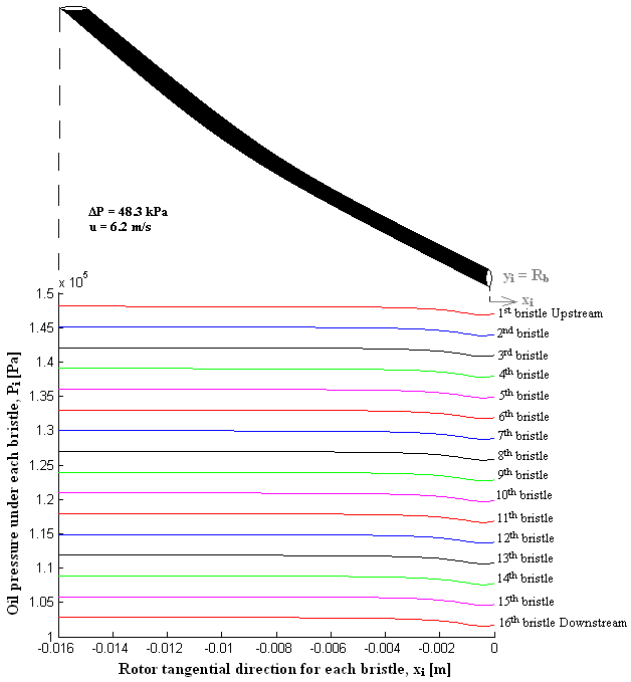

Figure 5 Oil pressure distributions along x_i for each bristle, ΔP = 48.3 kPa, u = 6.2m/s

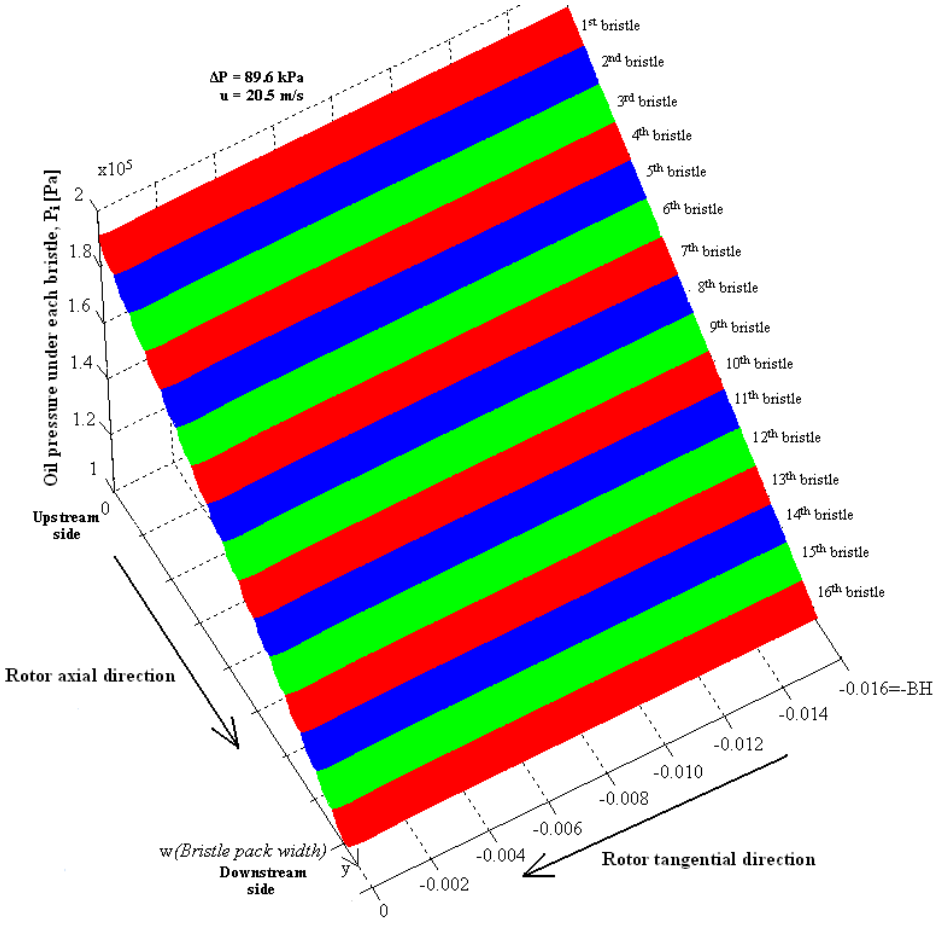

Figure 6 Oil pressure change under each bristle along rotor axial and tangential directions

In the previous studies by Duran et. al. [4, 5], analyses have been performed based on the control volume selection between the rotor surface and the entire bristle pack, and oil pressure distribution along *y*-axis *(rotor axial direction)* has been found almost linear. Therefore, linear pressure distribution was accepted by Duran et. al. [4] for the rotor axial direction. In this work, oil pressure has been developed based on the control volume selection as the oil under each bristle, and the pressure for each bristle depends on both of the local coordinates, x_i and y_i. Following from Fig. 6, comments on almost linear pressure distribution along rotor axial direction can be done. Mean value of oil pressure for each bristle with respect to x_i coordinate is developed in order to make comments on almost linear pressure distribution definite.

$$P_{i_{mean-x_i}}(y_i) = \frac{1}{BH}\int_{-BH}^{0} P_i(x_i, y_i)\cdot dx_i \tag{16}$$

P_i is the oil pressure under each bristle given in Eq. 15. Trapezoid rule is selected as a numeric integration method, and numeric integral is evaluated by writing a MATLAB code.

$$P_{i_{mean-x_i}}(y_i) = \frac{1}{BH}\int_{-BH}^{0} P_i(x_i, y_i)\cdot dx_i = \frac{1}{BH}\left\{\frac{l}{2}\cdot\left[P_i(x_{i_1}, y_i) + 2P_i\left(x_{i_1}+l, y_i\right) + \ldots + P_i\left(x_{i_2}, y_i\right)\right]\right\} \tag{17}$$

A step of numeric integration, *l*, is taken as *BH/1600*. In Fig. 7, mean-*x* pressure for the first bristle is given for 89.6 kPa pressure load and 20.5 m/s rotor surface speed. As it can be seen from the figure, pressure distribution along y_i-axis of the first bristle is almost linear. Pressure distribution along *y*-axis *(rotor axial direction)*, which is given in Fig. 8, can be obtained by combining local mean-x_i pressure distribution of each bristle in one row of the bristle pack.

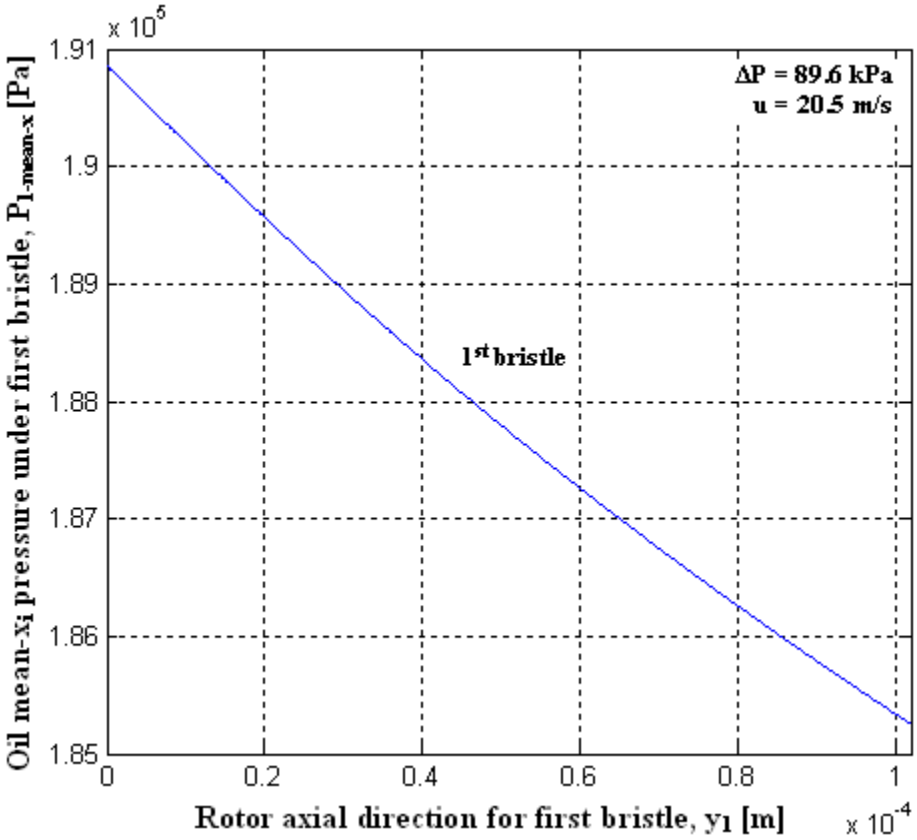

Figure7 Mean-x_i pressure change with rotor axial direction for the first bristle

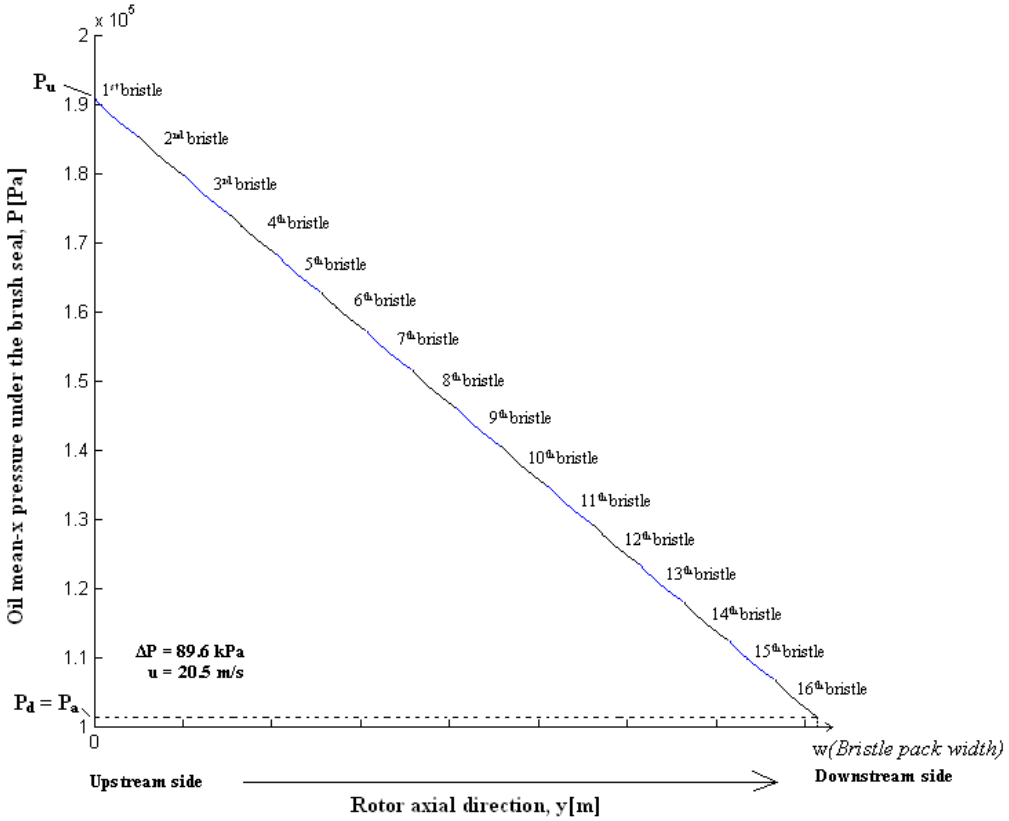

Figure 8 Mean-x pressure change with rotor axial direction for the bristle pack

As it can be seen from the Fig. 8, oil pressure change along rotor axial direction *(y-axis)*, which is found by combining local pressure distributions of Eq. 17 for each bristle, is almost linear. This result is consistent with applications as reported by Braun et al. [7].

V. Conclusion

Shear heating in brush seals is important as it affects the hydrodynamic lift clearance and lifting force. This in return, determines the seal leakage performance. Shear heat dissipation is also one of the reasons for stabilization of the lifting force after certain rotor speeds. Until now, suggested theories did not include the shear heating effect, or underestimated the frictional and blow down forces. In this study, effect of temperature to pressure distribution is calculated with the aid of temperature function derived in the previous studies [4]. Pressure distribution under the bristle pack is previously derived with the selection control volume as the volume under the bristle pack [5], and pressure distribution in rotor axial direction is found to be almost linear. In this study, pressure equations are derived by selecting the control volume as the oil under individual bristles, and consecutive boundary conditions are applied. Results of this analysis show almost linear pressure drop at the rotor axial direction, which is consistent with other observations [7] and previous analyses [4, 5]. Pressure change in circumferential direction shows similar distribution for each bristle, with different magnitudes. Evident change in oil pressure is observed at the projection of bristle portion at fence height region.

References

[1] Ingistov, S., "Power Augmentation and Retrofits of Heavy Duty Industrial Turbines model 7EA," Proceedings of Power-Gen International Conference, Las Vegas, NV, 2001.

[2] Bhate, N., Thermos, A.C., Aksit, M.F., Demiroglu, M., Kizil, H., "Non-Metallic Brush Seals For Gas Turbine Bearings", Proceedings of ASME Turbo Expo 2004, GT2004-54296, 2004.

[3] Aksit, M. F., Bhate, N., Bouchard, C., Demiroglu, M., and Dogu, Y., 2003, "Evaluation of Brush Seal Performance for Oil Sealing Applications," AIAA paper no. AIAA-2003-4695.

[4] Duran E. T., Aksit M. F., Dogu Y., "Effect of Shear Heat on Hydrodynamic Lift of Brush Seals in Oil Sealing," AIAA Paper No. AIAA-2006-4755, 2006.

[5] Duran, E. T.., Aksit, M. F., Dogu, Y., "Oil Temperature Analysis of a Brush Seal", IJTC-2007-44397.

[6] Aksit, M.F., Dogu, Y., J.A. Tichy and Gursoy M., "Hydrodynamic Lift of Brush Seals In Oil Sealing Applications," Proceedings of 40th AIAA/ASME/SAE/ASEE Joint Propulsion Conference & Exhibit, Fort Lauderdale, Florida, AIAA Paper AIAA-2004-3721, 2004.

[7] Braun, M.J., Canacci, V.A., and Hendricks, R.C, "Flow Visualization and Quantitive Velocity and Pressure Measurements in Simulated Single and Double Brush Seals," Trib. Trans., 34, pp 70-80, 1991